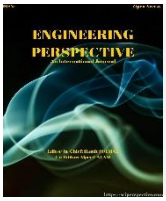

e-ISSN:2757-9077

ENGINEERING PERSPECTIVE

https://sciperspective.com/ Research Paper

Adaptive PID Controller Design for Velocity Control of a Hydrogen Internal Combustion Engines using RBF Neural Networks

Quang Truc Dam[1,*], Fatima Haidar[1]

[1] *Capgemini Engineering, Research & Innovation Direction, 12 rue de la Verrerie, 92190, Meudon, France*

ABSTRACT

Achieving precise velocity control in ICEs is crucial for optimizing performance, fuel efficiency, and reducing emissions. However, the nonlinear dynamics and uncertainties inherent in ICE systems pose significant challenges for conventional control methods. In this paper, we propose an adaptive approach integrating a Proportional-Integral-Derivative (PID) controller with Radial Basis Function Neural Networks (RBFNN) to address these challenges effectively. The proposed controller architecture comprises two main components: a RBFNN designed to estimate modeling uncertainties, such as unknown friction and external disturbances impacting the ICE structure, and a primary PID controller responsible for regulating velocity. The RBFNN serves as a dynamic estimator, continuously learning and adapting to variations in system dynamics, thereby enhancing the controller's robustness and adaptability. By accurately capturing the nonlinearities and uncertainties inherent in ICEs, the RBFNN contributes to improved control performance and stability. To validate the efficacy of the proposed approach, extensive numerical simulations are conducted using MATLAB Simulink. The simulations involve various operating conditions and scenarios to comprehensively evaluate the controller's performance. Additionally, the proposed methodology is compared against conventional PID methods documented in the literature to assess its superiority in terms of robustness, tracking accuracy, and disturbance rejection. The results demonstrate that the adaptive PID controller utilizing RBFNNs outperforms traditional PID approaches, exhibiting superior velocity regulation and disturbance rejection capabilities. Moreover, the proposed methodology showcases promising potential for real-world implementation in ICE-based systems, offering enhanced control performance and efficiency. Overall, this study contributes to advancing the field of control engineering by introducing a novel adaptive control strategy tailored specifically for velocity control in internal combustion engines, leveraging the capabilities of RBFNNs to mitigate uncertainties and improve overall system performance.

Keywords: Internal Combustion Engine (ICE); MATLAB-Simulink; Proportional-Integral-Derivative (PID); Radial Basis Function Neural Networks (RBFNN), Hydrogen.

History
Received: 19.04.2024
Accepted: 13.01.2025

How to cite this paper: Dam, Q.T., Haidar, F., (2025). Adaptive PID Controller Design for Velocity Control of a Hydrogen Internal Combustion Engines using RBF Neural Networks. Engineering Perspective, 5 (1), 41-48. http://dx.doi.org/10.29228/eng.pers.76280

Author Contacts
**Corresponding Author*
e-mail addresses :Quang-truc.dam@capgemini.com , Fatima.haidar@capgemini.com ,

1. Introduction

The internal combustion engine (ICE) stands as a pinnacle of modern engineering, revolutionizing transportation, and power generation since its inception [1-3]. It represents a marvel of human innovation, converting the chemical energy stored in fossil fuels into mechanical energy through controlled combustion within a confined space. Among the various types of internal combustion engines, the four-stroke internal combustion engine emerges as a cornerstone in automotive and industrial applications, owing to its efficiency, reliability, and versatility.

Four-stroke internal combustion engines operate on a systematic cycle of intake, compression, power, and exhaust strokes, each meticulously orchestrated to harness energy from fuel and propel machinery forward. This cyclic process not only ensures optimal power output but also minimizes waste and environmental impact compared to alternative engine designs.

Four-stroke internal combustion engines are predominant choices in the field of conventional and hybrid vehicles due to their superior energy efficiency compared to two-stroke engines [1-3]. This preference stems from multiple factors, including the fact that a four-

stroke engine generates power only once every two revolutions, resulting in lower fuel consumption compared to two-stroke engines, which require one revolution for a complete power stroke. This fundamental difference in how four-stroke and two-stroke engines generate power has significant implications in terms of fuel economy and emission reduction.

Four-stroke engines also offer the additional advantage of producing fewer emissions and providing a more constant torque than their two-stroke counterparts. This is attributable to the more complex design of four-stroke engines, which allows them to optimize the combustion process and minimize energy losses.

Regarding spark ignition (SI) engines, they primarily operate on gasoline, although they can also use ethanol as an alternative fuel, making them more energy versatile. The main components of SI engines include the intake and exhaust manifold, intake and exhaust valves, spark plug, piston, coolant, cylinder, crankcase, connecting rod, and crankshaft. Each component plays a crucial role in the overall operation of the engine, contributing to its performance and efficiency.

In this study, we extend the scope of conventional internal combustion engine technology by adapting it for hydrogen fuel utilization. Hydrogen, as a clean and sustainable energy carrier, offers a compelling alternative to fossil fuels, enabling combustion with zero carbon emissions. Unlike traditional hydrocarbon-based fuels, hydrogen combustion primarily produces water vapor, significantly reducing greenhouse gas emissions and contributing to environmental sustainability. The adaptation of internal combustion engines to hydrogen fuel presents unique challenges, including optimizing fuel injection strategies, mitigating pre-ignition risks, and ensuring efficient combustion dynamics. By leveraging advanced control methodologies, we aim to develop an adaptive speed control system tailored for hydrogen-powered ICEs, enhancing their performance, stability, and efficiency. This transition toward hydrogen-based internal combustion engines aligns with global efforts to decarbonize transportation and industrial applications while preserving the advantages of well-established ICE technology.

Motivated by its widely used in many applications, the study of controlling this motor. The design of speed controller for internal combustion engines (ICE) has garnered much attention in the automation community due to its crucial role in improving engine performance and efficiency. In recent studies [4-5], researchers have focused on implementing PID controllers specifically tailored to control the speed of ICEs. These controllers offer a robust and versatile solution to maintain desired speeds under various operating conditions, thereby contributing to enhancing engine operation and energy efficiency.

In another notable initiative [6], a sophisticated control system designed for engine speed and torque, using a linear quadratic regulator (LQR) approach, was introduced. This system employs first-order transfer functions with delay, demonstrating successful implementation and validation across the operational spectrum of both diesel and spark ignition engine dynamometer sets [7]. The use of LQR methodology underscores the importance of advanced control techniques in optimizing engine performance and ensuring smooth operation under diverse load conditions.

Furthermore, the application of Model Predictive Control (MPC) has proven to be a promising avenue for enhancing the accuracy and adaptability of speed control systems for ICE [8-10]. In [11] an adaptive sliding mode controller is proposed for controlling the air-fuel ratio of an ICE. Moreover, in a recent breakthrough [12], deep learning methodologies were integrated into the MPC controller design process, demonstrating the potential of innovative techniques in optimizing engine performance and efficiency. Additionally, the exploration of Secure Deep Reinforcement Learning (SDRL) in [13] highlights ongoing efforts to develop robust and reliable control strategies capable of ensuring both optimal performance and operational safety of ICE operations. These diverse approaches collectively contribute to advancing the state of the art in speed control systems for internal combustion engines, offering insights and innovative solutions to optimize engine performance and enhance overall operational efficiency.

Motivated by these works, in this paper, one shall propose another approach using the advantage of radial basic functional neural network for design an adaptive PID controller for speed control of an ICE.

2. Dynamic model of an H_2-ICE

The key components of internal combustion engines can be analyzed to enhance understanding of their operation and interrelation. This deepens the knowledge base of engineers and researchers, paving the way for technological advancements and improvements in engine design and energy efficiency. To simplify the control design process, the dynamic model of an internal combustion engine (ICE) can be divided into two sub-dynamic models. First, the combustion dynamics, which include all the equations describing processes from air and fuel intake via the environment and fuel injectors to the combustion process. This process generates engine torque, which drives the crankshaft. Second, the crankshaft dynamic model, where the engine torque serves as an input for rotating the crankshaft. This rotation represents the motion of the ICE, with engine speed corresponding to the rotation speed of the crankshaft.

2.1. Combustion Dynamic Model

The combustion model starts by taking the air from the environment to send to the chamber, this controls the amount of air flowing into the engine in response to the driver's accelerator pedal action.

The mass flow rate ($\dot{m}_{air}$) is determined as following Eq. (1) [14]:

$$\dot{m}_{air} = \frac{A_{eff} P_{upstr}}{\sqrt{R T_{upstr}}} \Psi(P_{ratio}) \quad (1)$$

Where P_{ratio} is the ratio of downstream pressure (P_{dowstr}) and upstream pressure (P_{upstr}).

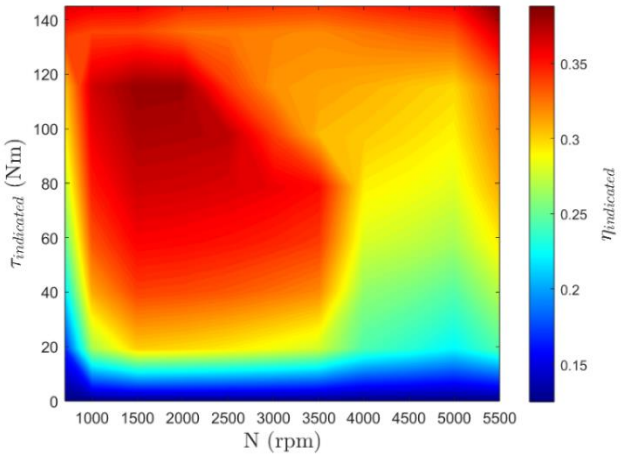

Figure 1. Charging Efficiency Coefficient [20].

$$\Psi(P_{ratio}) = \begin{cases} \sqrt{\gamma\left(\frac{2}{\gamma+1}\right)^{\frac{\gamma+1}{\gamma-1}}} & if:\ P_{ratio} < \left(\frac{2}{\gamma+1}\right)^{\frac{\gamma}{\gamma-1}} \\ \sqrt{\frac{2\gamma}{\gamma-1}\left(P_{ratio}^{\frac{2}{\gamma}} - P_{ratio}^{\frac{\gamma+1}{\gamma}}\right)} & if: \left(\frac{2}{\gamma+1}\right)^{\frac{\gamma}{\gamma-1}} < P_{ratio} < P_{lim} \\ \frac{P_{ratio}-1}{P_{lim}-1}\sqrt{\frac{2\gamma}{\gamma-1}\left(P_{lim}^{\frac{2}{\gamma}} - P_{lim}^{\frac{\gamma+1}{\gamma}}\right)} & if: P_{lim} < P_{ratio} \end{cases} \quad (2)$$

Where $P_{upstr} = P_{abt} = 101325$ Pa is the ambient pressure. $\Psi(P_{ratio})$ is the based follow correlation and is the function of P_{ratio} calculates the based on the different conditions of flow.

$$P_{ratio} = \frac{P_{dowstr}}{P_{upstr}} \quad (3)$$

Where P_{lim} is the pressure ratio limitation, $\gamma = 1.4$ is the ratio of specific heats

A_{eff} is the effect area, and is calculated as follows:

$$A_{eff} = \frac{\pi}{4} {D_{thr}}^2 C_{thr}(\theta_{thr}) \quad (4)$$

$$\theta_{thr} = \Theta_{ct\_thr}\frac{90}{100} \quad (5)$$

Where θ_{thr} is the open angle of the throttle valve(in degree), Θ_{ct_thr} is the percentage of throttle body that open, D_{thr} is the throttle diameter at opening, $C_{thr}(\theta_{thr})$is the discharge coefficient. To calculate the fuel flow in the hydrogen (H_2) internal combustion engine, one utilizes the characteristics of the fuel injector along with the fuel injector pulse-width. The model for fuel flow is expressed as:

$$\dot{m}_{fuel} = \frac{NS_{inj}P_{winj}N_{cyl}}{c_{ps}1000 * 60} \quad (6)$$

Where N represents engine speed in rpm, S_{inj} denotes the fuel injector slope, N_{cyl} signifies the number of engine cylinders, c_{ps} stands for the crankshaft revolutions per power stroke.

In the SI engine the indicated torque means that the torque or power of the engine is evaluated in the scope of thermodynamics (pressure and volume of cylinder), not including any mechanical losses in the whole power development and transmission process conceptually illustrates pressure variation in a cylinder along with crankshaft rotation angle. This torque is calculated as follows [11]:

$$\tau_{indicated} = \frac{P_{indicated} * 60}{2\pi N} \quad (7)$$

Where $P_{indicated}$ is the indicated power and can be calculated as:

$$P_{indicated} = \dot{m}_{fuel} * LHV\eta_{indicated} \quad (8)$$

Where $\eta_{indicated}$ is the engine indicated load efficiency as well as a function of engine speed (N) and indicated torque ($\tau_{indicated}$) as depicted in Figure 1

2.2. Crankshaft Model

The Crankshaft model demonstrates the indicated torque generated by the combustion reaction inside the chamber acts on the crankshaft, which then case the movement of crankshaft, hence generate the rotation movement of ICE. This relation is described as in the following equation:

$$\dot{\omega}(t) = -J^{-1}S(\omega)J\omega + J^{-1}(\tau_{control} + \tau_{uncertainties}) \quad (9)$$

Where ω is the rotation rate of the ICE, J is the crankshaft's moment of initial, $\tau_{control}$ is the indicated torque, $\tau_{uncertainties}$ is the unknown factor such as friction, engine load.

Because the crankshaft rotate in single axe, then we have $-J^{-1}S(\omega)J\omega = 0$, now set $\Gamma = J^{-1}\tau_{uncertainties}$, then we have the new dynamic equation of ICE is as:

$$\dot{\omega}(t) = J^{-1}\tau_{control} + \Gamma \quad (10)$$

3. Controller Design

In the previous section, we have developed the model of ICE H2 as well as its mathematical model. In this section, we shall focus on develop a controller for controlling the velocity of the ICE using Fuel injector pulse-width and Throttle valve's angle as control input.

Unlike the direct control scheme, using injector pulse-width and Throttle valve's angle as control input require a cascade control structure to control the velocity of ICE.

The controller structure is given in Figure. 2. The controller consist of two controllers, namely Inner loop controller and outer loop controller. The outer loop controller will be in charge of calculating the needed torque for controlling the velocity of ICE, this value then will be considered as desired value for the inner loop controller. The inner controller then uses the calculated torque valued given by the outer controller to calculate the needed injector pulse-width ($average\ value$) and Throttle valve's angle for obtaining the desired torque. It is worth noting that, using the cascade structure requires the inner controller loop responses faster than the outer control loop.

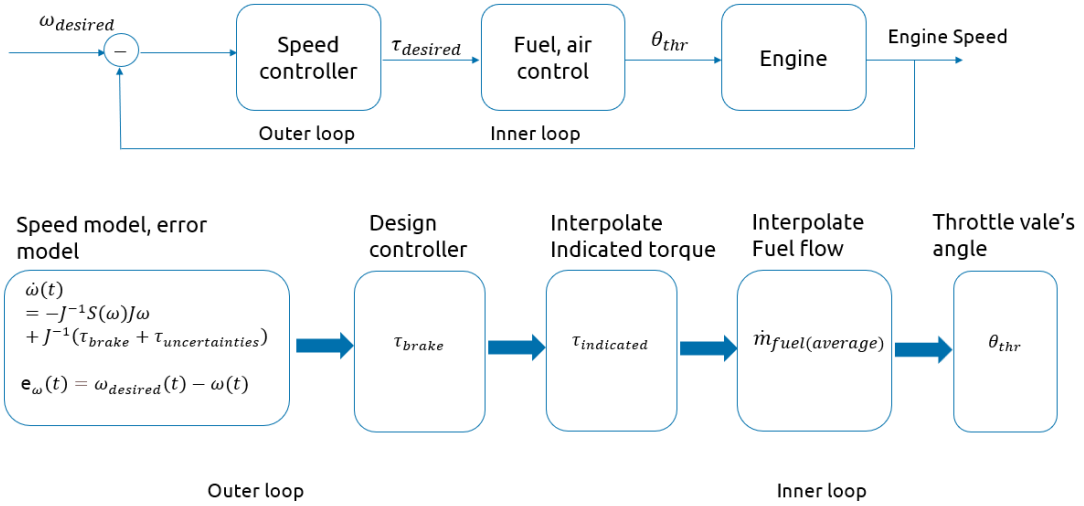

Figure 2. Control structure of ICE velocity controller.

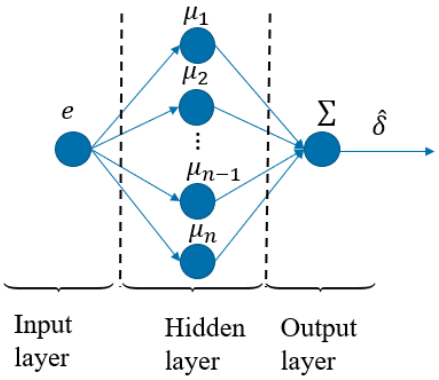

Figure 3. RBF neural network structure.

3.1. Outer loop controller

The objective of the outer controller to calculate the request torque based on the desired rotation velocity of the crankshaft.

Now let us define the controller tracking error as following:

$$e = \omega_{desired} - \omega \tag{11}$$

From (10,11) one gets:

$$J\dot{e} = -\tau_{control} - J\Gamma + J\dot{\omega}_{desired} \tag{12}$$

Let's define now $\delta = -J\Gamma + J\dot{\omega}_{desired}$ then (12) can be rewritten as follow:

$$J\dot{e} = -\tau_{control} + \delta \tag{13}$$

Remark 1: Taking into account that the function δ is unknown, the control input $\tau_{control}$ cannot be derived directly from (13). To overcome this drawback, an artificial neural network using RBFNN will be employed to estimate the unknown function δ.

For this sake, we propose to use the RBF neural network for estimating the value of δ ($\hat{\delta}$), The model of this neural network is given in Figure 4.

The RBFNN structure consists of three layers, namely the input, the output, and the hidden layer.

- Input Layer: The input to the network is the error signal, denoted as e. This signal is propagated to the hidden layer.
- Hidden Layer: The hidden layer contains n radial basis neurons, each corresponding to a radial basis function (RBF). These neurons compute the response to the input using a Gaussian activation function, which is defined as:

$$\mu_i(e) = exp\left(-\frac{\|e - r_i\|}{\eta_i}\right) \tag{14}$$

where r_i is the center of the radial basis function for neuron i, and η_i is the width of the Gaussian function. The output of the hidden layer can be represented as:

$$\mu(e) = [\mu_1(e) \quad \cdots \quad \mu_n(e)]^T \tag{15}$$

- Output Layer: The output layer produces the final output δ, which is a weighted sum of the hidden layer activations, plus an approximation error term e_{rbf}. Mathematically, this is expressed as:

$$\delta = W\mu(e) + e_{rbf} \tag{16}$$

Where W is the ideal weigh matrix and e_{rbf} is the approximation error. Based on the neural network theory, since the number of nodes is chosen suitable, this approximation error will be bounded. However, the ideal weigh matric (W) is unknown, therefore, for calculating the estimation of Γ one needs to estimate the value of W, this estimation is given as $\widehat{W}$, Hence the estimation of δ is given as:

$$\hat{\delta} = \widehat{W}\mu(e) \tag{17}$$

Based on this estimation, we propose the Robust controller using the Lyapunov theorem as follows:

$$\tau_{control} = K_1 e + K_2 \int e dt + K_3 sign(e) + \hat{\delta} \quad (18)$$

Assumption 1: The function δ is smooth and bounded.

Assumption 2: The neural network estimation error e_{rbf} is assumed to be small, unknown, and bounded by the following bounds:

$$\exists \epsilon_{erbf} \ll, \in \mathbb{R}^+, \max_{t \geq 0} \left\| e_{rbf} \right\| \leq \epsilon_{erbf} \quad (19)$$

Theorem 1: Consider the system (10) under the assumption 1,2. If the controller gains are design such as:

$$K_1, K_2 > 0; \;\; K_3 > \epsilon_{erbf} \quad (20)$$

And the estimation of weight matrix is designed such as:

$$\dot{\widehat{W}} = \mu(e) e \quad (21)$$

Then the stability of the controller will be ensured, which lead to the tracking control error e will converge to zero exponentially.

Remark 2: This approach separates all unidentified factors and model parameters from the control signal, enabling us to develop the controller independently. A similar technique is described in [15]. It's important to mention that besides employing Neural Networks (NN) for handling unknown factors, another commonly utilized method involves using observers to estimate these unknown factors, as explained in [16-19].

Remark 3: The controller suggested in this study, as shown in Eq. (18) and Eq. (21), operates regardless of the model parameters. Consequently, it can be applied to various systems beyond just Internal Combustion Engine (ICE) systems.

The proof of this theorem will be given in the following equations. Let us define $\widetilde{W} = W - \widehat{W}$ and $\tilde{\delta} = \delta - \hat{\delta}$, from Eq. (17) and Eq. (18) one gets:

$$\tilde{\delta} = \widetilde{W} \mu(e) + e_{rbf} \quad (22)$$

Consider the follows Lyapunov function:

$$V = \frac{1}{2} J e^2 + \frac{1}{2} K_2 \left(\int e dt \right)^2 + \frac{1}{2} tr\left(\widetilde{W}^T \widetilde{W} \right) \quad (23)$$

From Eq. (13), Eq. (18), Eq. (21), Eq. (26) one gets:

$$\begin{aligned} \dot{V} &= e\left(-K_1 e - K_2 \int e dt - K_3 sign(e) + \delta - \hat{\delta} \right) \\ &\quad + K_2 e \int e dt - \; tr\left(\widetilde{W}^T \dot{\widehat{W}} \right) \\ &= e\left(-K_1 e - K_2 \int e dt - K_3 sign(e) + \widetilde{W} \mu(e) \right. \\ &\quad \left. + e_{rbf} \right) + K_2 e \int e dt \\ &\quad - \; tr\left(\widetilde{W}^T \mu(e) e \right) \end{aligned} \quad (24)$$

Taking into account the fact that $e\widetilde{W}\mu(e) - \; tr\left(\widetilde{W}^T \mu(e) e\right) = 0$. From (19) and (20) one gets: $e\left(e_{rbf} - K_3 sign(e)\right) \leq 0$. Hence, one can derive:

$$\dot{V} \leq -K_1 e^2 \leq 0 \quad (25)$$

3.2. Inner loop controller (Torque controller)

Based on the Eq. (6) to Eq. (8) we can derive the desired fuel mass flow rate as follows:

$$\dot{m}_{fuel} = \frac{\tau_{control} 2\pi N}{60 LHV \eta_{indicated}} \quad (26)$$

Based on Eq. (7), we can then determine the desired air mass flow rate as follows:

$$\dot{m}_{air} = \dot{m}_{fuel} AFR \quad (27)$$

Then the desired effect area is determined based on Eq. (2) as follows:

$$A_{eff} = \frac{\dot{m}_{air} \sqrt{R T_{upstr}}}{P_{upstr} \Psi(P_{ratio})} \quad (28)$$

Hence, based on Eq.(6), the desired open angle of throttle valve is given as:

$$\theta_{thr} = C_{thr}^{-1} \left(\frac{4 A_{eff}}{\pi {D_{thr}}^2} \right) \quad (29)$$

4. Results and Discussion

In this section, a simulation validation of our proposed controller will be carried out using MATLAB Simulink. The main goal of these simulations is to demonstrate the effectiveness of our controller in terms of handling the effect of the external unknown disturbances as well as the parametric uncertainties which may affect outer loop model. Then a comparison with the classic PID controller is considered The parameters of ICE using in this simulation is given in Table 1.

Table 1. Parameter of ICE.

Parameters	Values	Units
T_{upstr}	300	K
P_{upstr}	101325	Pa
R	287	J/(kg*K)
γ	1.4	-
D_{thr}	50	mm
S_{inj}	6.4516	mg/ms
LHV	47300000	J/kg
N_{cyl}	4	-
c_{ps}	2	rev/stroke

4.1. PID controller design

To design the PI controller for controlling the crankshaft dynamics, as governed by Eq. (10), we utilized pidtune provided by MATLAB. This tool facilitated the automatic tuning of the PI controller parameters, providing an optimized response for the system. Through this process, we ensured that the PI controller achieved the desired balance between stability, response time, and error minimization for the crankshaft control. The results PID tuner tool

gives the following results for the PI controller ($K_p = K_1 = 6.666$, $K_i = K_2 = 1.167$).

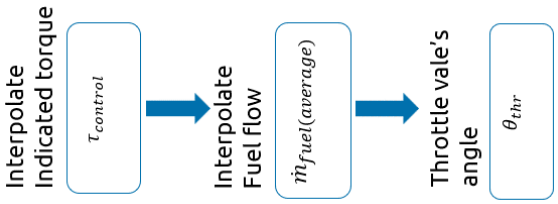

Figure 4. Torque control diagram.

4.2. Simulation results

The objective of this study is to analyze the speed tracking performance of the proposed controller in comparison to a conventional PID controller, particularly under the influence of disturbances. A combination of step and sinusoidal reference signal (Figure 5) were selected to evaluate the controller's performance across various dynamic conditions. The step signal simulates a sudden change in system demands, reflecting typical scenarios in real-world engine control systems where abrupt shifts in load or speed occur. In contrast, the sinusoidal component tests the controller's ability to track a continuously varying signal, mimicking situations where engine speed gradually fluctuates, such as during acceleration and deceleration cycles. This input aims to assess the system's robustness and adaptability under both steady-state and transient operating conditions. The engine's performance is evaluated under conditions of friction and external disturbances. Specifically, the friction effects impacting the engine are depicted in Figure 6, while the external disturbances, including factors such as environmental variations and load changes, are shown in Figure 7. These figures represent the challenges the controllers must overcome to maintain accurate speed tracking. The study aims to demonstrate the effectiveness of the proposed controller in managing these disturbances, ensuring superior speed tracking performance when compared to the traditional PID controller.

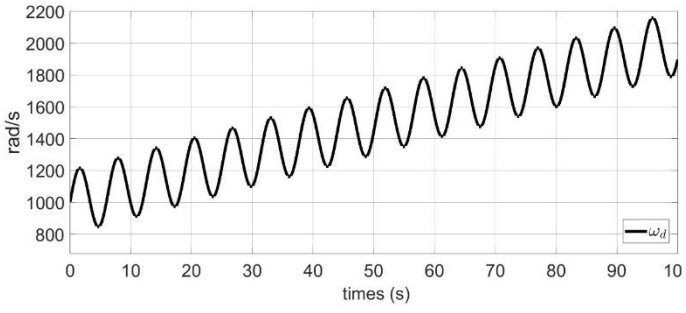

Figure 5. Desired value for controller design.

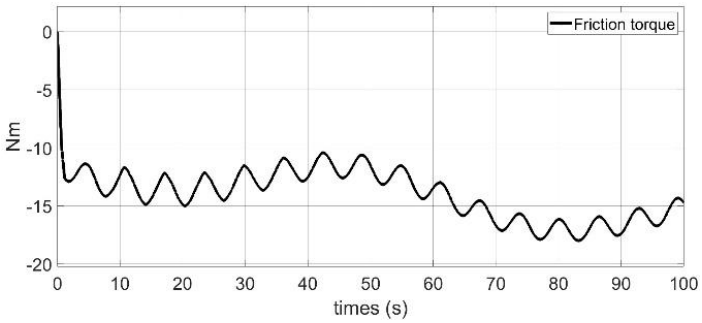

Figure 6. The friction affected to the system (10) during the simulation.

The tracking control performances of both the PID and the PID RBFNN, proposed in this study, are showcased in Figures 8 and 9. These figures demonstrate that all proposed controllers successfully fulfill the trajectory tracking task. However, a noticeable disparity emerges in the effectiveness between the PID and the proposed method. Specifically, the results from the PID exhibit less efficiency compared to the proposed approach. It becomes evident that the controller suggested in this study enables the maintenance of the ICE at the desired speed with a relatively minimal tracking error. This observation underscores the superior performance of the proposed method in ensuring precise speed control, highlighting its potential for enhancing operational stability and efficiency within the ICE system.

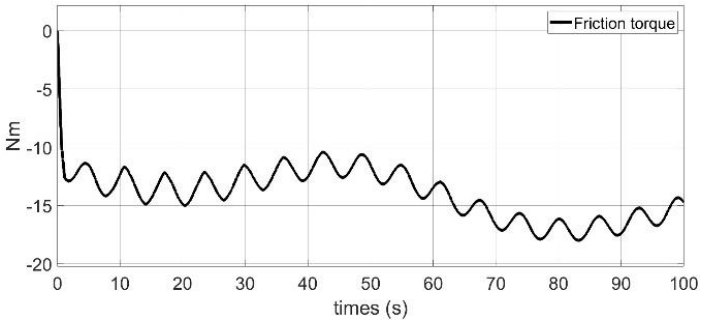

Figure 7: The external disturbance torque affected to the system (10) during the simulation.

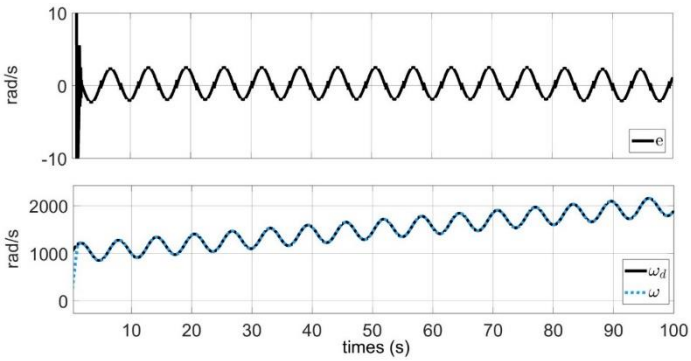

Figure 8: Simulation results for velocity tracking using RBFNN PID controller.

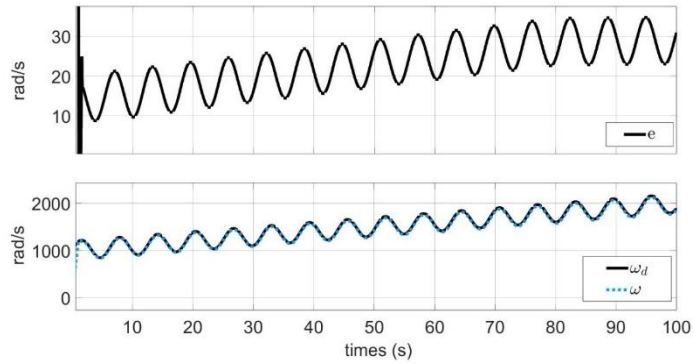

Figure 9. Simulation results for velocity tracking using classical PID controller.

Figure 10 illustrates the output torque of the Internal Combustion Engine (ICE) compared to its desired value derived from equation (18). This depiction showcases the effectiveness of our method in achieving precise torque control, ensuring consistency and accuracy in torque regulation. The close alignment between actual and desired torque values signifies the method's robustness. This precise torque control facilitates smooth speed tracking within the ICE system, enhancing operational efficiency and performance stability. Thus, Figure 10 serves as visual evidence of our method's ability to regulate torque output effectively, leading to improved speed tracking and overall system performance in ICE applications.

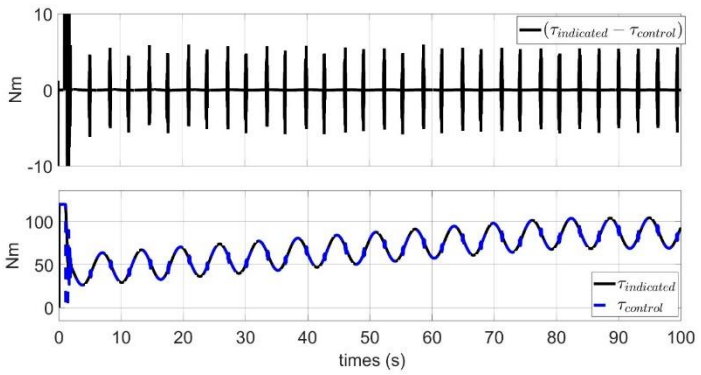

Figure 10. Engine torque and its desired value using RBFNN PID controller.

5. Conclusions

This paper proposed an adaptive controller for speed control on an ICE subject to bounded disturbances, model uncertainties and unknown parameters. The controller law is designed based on the PID technique. The unknown part is estimated using adaptive neural network using radius basic functional technique. The relevance of our proposed method, in terms of compensating the effects resulting from the disturbance, model uncertainties and unknown parameters, have been demonstrated through simulation results performed on the ICE system. To show the performance of our proposed observer, a comparison with the classic PID controller is conducted.

Acknowledgment

This work was carried out at Altran Prototypes Automobiles (APA) as a part of the Intelligence & Innovation Powertrain project within the Capgemini Engineering Research and Innovation Department.

Conflict of Interest Statement

Q-T.D and F.H contributed equally. All authors have given approval to the final version of the manuscript. The authors declare that there is no conflict of interest in the study. The authors would also like to thank Guillaume Guilbert who have contributed immensely for the part of the project.

CRediT Author Statement

Quang Truc Dam: Writing original draft & formal analysis - review & editing, supervision, project administration & validation. **Fatima Haidar:** Review & validation.

References

1. Ehsani, M., Gao, Y., Longo, S., & Ebrahimi, K. (2018). Modern electric, hybrid electric, and fuel cell vehicles (3rd ed.). CRC Press.
2. Stone, R. (1992). Introduction to internal combustion engines (2nd ed.). The Macmillan Press LTD.
3. Heywood, J. B. (2018). Internal combustion engine fundamentals (2nd ed.). McGraw-Hill Education.
4. Nise, N. S. (2015). Control systems engineering (7th ed.). Wiley.
5. Gao, D., Lei, Y., Zhu, H., & Ni, J. (2015). Constant speed control of four-stroke micro internal combustion swing engine. Chinese Journal of Mechanical Engineering, 28(5), 971–982. https://doi.org/10.3901/CJME.2015.0512.070
6. López, J. D., Espinosa, J. J., & Agudelo, J. R. (2011). LQR control for speed and torque of internal combustion engines. IFAC Proceedings Volumes, 44(1), 2230–2235. https://doi.org/10.3182/20110828-6-IT-1002.02176
7. Norouzi, A., Heidarifar, H., Shahbakhti, M., Koch, C. R., & Borhan, H. (2021). Model predictive control of internal combustion engines: A review and future directions. Energies, 14(19), 6251. https://doi.org/10.3390/en14196251
8. Gordon, D. C., et al. (2022). End-to-end deep neural network based nonlinear model predictive control: Experimental implementation on diesel engine emission control. Energies, 15(24), 9335. https://doi.org/10.3390/en15249335
9. Di Cairano, S., Doering, J., Kolmanovsky, I. V., & Hrovat, D. (2014). Model predictive control of engine speed during vehicle deceleration. IEEE Transactions on Control Systems Technology, 22(6), 2205–2217. https://doi.org/10.1109/TCST.2014.2309671
10. Norouzi, A., Heidarifar, H., Shahbakhti, M., Koch, C. R., & Borhan, H. (2021). Model predictive control of internal combustion engines: A review and future directions. Energies, 14(19), 6251. https://doi.org/10.3390/en14196251
11. Souder, J. S., & Hedrick, J. K. (2004). Adaptive sliding mode control of air–fuel ratio in internal combustion engines. International Journal of Robust & Nonlinear Control, 14(6), 525–541. https://doi.org/10.1002/rnc.901

12. Norouzi, A., et al. (2022). Deep learning-based model predictive control for compression ignition engines. arXiv preprint. https://doi.org/10.48550/ARXIV.2204.00139
13. Norouzi, A., Shahpouri, S., Gordon, D., Shahbakhti, M., & Koch, C. R. (2023). Safe deep reinforcement learning in diesel engine emission control. Proceedings of the Institution of Mechanical Engineers, Part I: Journal of Systems and Control Engineering, 237(8), 1440–1453. https://doi.org/10.1177/09596518231153445
14. Heywood, J. B. (1988). Internal combustion engine fundamentals. McGraw-Hill.
15. Dam, Q. T., Thabet, R. E. H., Ali, S. A., Guerin, F., & Tang, Y. (2023, September 27). Adaptive neural network-based sliding mode controller for trajectory tracking of a quadrotor UAV. TechRxiv. https://doi.org/10.36227/techrxiv.24174771.v1
16. Dam, Q. T., Thabet, R. E. H., Ali, S. A., Guérin, F., & Ghani, H. A. (2023). A high-gain observer design for nonlinear system with delayed measurements: Application to a quadrotor UAV. IFAC-PapersOnLine, 56(2), 6739–6744. https://doi.org/10.1016/j.ifacol.2023.10.379
17. Dam, Q. T., Thabet, R. E. H., Ali, S. A., & Guerin, F. (2024). Observer design for a class of uncertain nonlinear systems with sampled-delayed output using high-gain observer and low-pass filter: Application for a quadrotor UAV. IEEE Transactions on Industrial Electronics, 71(1), 933–942. https://doi.org/10.1109/TIE.2023.3247786
18. Dam, Q. T., Thabet, R. E. H., Ali, S. A., & Guerin, F. (2022, June). Filtered high-gain observer design for a class of nonlinear systems subject to delayed measurements: Application to a quadrotor UAV. 2022 American Control Conference (ACC), Atlanta, GA, USA. IEEE. https://doi.org/10.23919/ACC53348.2022.9867537
19. Dam, Q. T., Thabet, R. E. H., Ali, S. A., Guérin, F., & Hugo, A. (2021, June). Continuous–discrete time high gain observer design for state and unknown inputs estimations of quadrotor UAV. 2021 European Control Conference (ECC), Delft, Netherlands. IEEE. https://doi.org/10.23919/ECC54610.2021.9655232
20. Dam, Q. T., Haidar, F., Mama, N., & Chennapalli, S. J. (2024). Modeling and simulation of an internal combustion engine using hydrogen: A MATLAB implementation approach. Engineering Perspective, 4(3), 108–118. http://dx.doi.org/10.29228/eng.pers.76219